ARTICLE IN PRESS

Pervasive and Mobile Computing ▮ (▮▮▮▮) ▮▮▮–▮▮▮

Contents lists available at ScienceDirect

Pervasive and Mobile Computing

journal homepage: www.elsevier.com/locate/pmc

Indoor positioning via subarea fingerprinting and surface fitting with received signal strength

Bang Wang [a,*], Shengliang Zhou [a], Laurence T. Yang [b,c], Yijun Mo [a]

[a] School of Electronic Information and Communications, Huazhong University of Science and Technology (HUST), Wuhan, China
[b] School of Computer Science and Technology, Huazhong University of Science and Technology (HUST), Wuhan, China
[c] Department of Computer Science, St. Francis Xavier University, Antigonish, Canada

ARTICLE INFO

Article history:
Received 22 January 2015
Received in revised form 6 June 2015
Accepted 16 June 2015
Available online xxxx

Keywords:
Indoor localization
Fingerprinting
Surface fitting
Subarea division and determination
Location search

ABSTRACT

The fingerprinting technique based on received signal strength (RSS) has been intensively researched for indoor localization in the last decade. Instead of using discrete reference points to build fingerprint database, this paper applies the surface fitting technique to construct RSS spatial distribution functions and proposes two location search methods to find the target location. We also propose to use subarea division and determination scheme to improve the fitting accuracy and search efficiency. In the offline phase, we divide the whole indoor environment into several subareas, construct a fingerprint for each subarea, and build a RSS distribution fitting function for each access point in each subarea. In the online phase, we first determine to which subarea a target belongs, and then search its location according to the proposed exhaustive location search or gradient descent based search algorithm. We conduct both extensive simulations and field experiments to verify the proposed scheme. The experiment results show that for the same reference point granularity, the proposed localization scheme can achieve about 22% localization accuracy improvement, compared with the classical nearest neighbor-based fingerprinting method.

1. Introduction

Indoor location information has been becoming more and more important for location-based applications and services. Some indoor localization technologies have been developed, which have different hardware requirements and localization accuracies. Due to the wide deployment of *wireless local area networks* (WLANs) as indoor access systems, indoor localization based on the *received signal strength* (RSS) from *access point* (AP) has become a hot research topic in recent years [1,2].

Fingerprinting is the most popular distance-free indoor localization technique [3–6]. Generally, it is composed of two phases: the offline training phase and online positioning phase. For a given indoor environment, the RSS profiles of some predetermined *reference points* (RPs) with known coordinates are measured, processed and stored as fingerprints in the offline phase. In the online phase, the RSS profile of a mobile device is used to produce its own fingerprint that will be compared with those pre-stored fingerprints to determine its location. A widely used positioning method is to select the location of a RP with the minimum fingerprint difference as the estimated location for the mobile device.

The performance of fingerprinting methods is dependent on the number of RP per unit area, viz the RP granularity. It has been reported that in general, increasing the number of RP per unit area helps to improve localization accuracy [3,7].

* Corresponding author.
E-mail addresses: wangbang@hust.edu.cn (B. Wang), zhoushengliang100@126.com (S. Zhou), ltyang@gmail.com (L.T. Yang), moyj@hust.edu.cn (Y. Mo).

http://dx.doi.org/10.1016/j.pmcj.2015.06.011
1574-1192/

However, the RSS measurements are very time-consuming and labor-intensive, and using more RPs will increase lots of the workloads and costs for localization.

Some approaches have been proposed to reduce the training efforts, while trying to maintain satisfactory localization accuracy [7–12]. Some propose to exploit unlabeled data, such as measurements of user casual movement traces, to improve the calibration of RSS distributions, when the field calibration data from reference points are insufficient [8–11]. Another approach is to create some virtual reference points and obtain their fingerprints by interpolating the fingerprints of nearby training locations [7,11,12]. Although these methods help to improve the localization accuracy with reduced training efforts, they are still a kind of discrete approach. Because their fingerprint comparison space is represented by some discrete yet limited reference points, unlabeled data or virtual reference points.

In this paper, we propose to use the surface fitting technique to generate fingerprint for an arbitrary indoor space point. This is done by constructing continuous RSS spatial distribution functions only from a few RP fingerprints. Such a fitting function describes the indoor RSS characteristics and only requires a few number of function coefficients. For example, let $\phi_j(x, y)$ denote the RSS from the jth AP at the space point (x, y). After we obtain ϕ_j for all available APs, we then construct a fingerprint for (x, y). Despite its simplicity, it is rather effective and can achieve much satisfactory localization accuracy. Furthermore, we apply a subarea division and determination scheme for surface fitting and location search. The basic idea is to divide the indoor environment into some subareas, say for example, according to walls and rooms. As rooms are often divided by concrete that generally introduces noticeable radio attenuations, we propose and use rooms as subareas in this paper. In each subarea, we create a subarea fingerprint and construct fitting functions based on the fingerprints of those RPs only within the subarea. The subarea division scheme is needed because it helps to improve fitting functions' accuracies. Furthermore, the use of subarea division scheme for localization not only helps to reduce the online comparison computations, but also provides a coarse positioning service for those applications with low positioning accuracy requirement.

In this paper, we propose two location search algorithms to find the location of a mobile device after subarea determination, namely, exhaustive location search (ELS) and gradient descent location search (GLS). Both are to minimize the fingerprint difference between the mobile device and a space point within the subarea. The former is to divide the subarea into many grid points (more than the number of RPs within the subarea) and compute their fingerprints based on the surface fitting functions built before. The latter is to iteratively search the global minimizer for an objective function of fingerprint difference. It utilizes the slope characteristics of the objective function by setting the negative gradient descent direction as the search direction, and it also applies an adjustable step size in the iterative search process. We have conducted extensive simulations and field experiments. The results show that on average 10% and 22% improvement of localization accuracy for the two proposed algorithms can be achieved, compared with the traditional fingerprinting algorithm.

The rest of this paper is organized as follows: Section 2 briefly gives the related work about fingerprint-based localization. Sections 3 and 4 give the offline work and online work of our method respectively. In Section 5, we conduct both simulations and field test experiments to verify our algorithm. Finally, we conclude this paper in Section 6.

2. Related work

Generally, fingerprint-based localization can be divided into two kinds: deterministic method [13,14] and probabilistic method [11,14–16]. For the former, it is to find a RP with the minimum fingerprint difference to the mobile fingerprint, for example, the nearest neighbor algorithm (NN) [14]. For the latter, it is to find a RP at which the mobile target is most likely appeared based on a probability distribution function (PDF) [13]. Most of these methods are a kind of discrete scheme. That is, all the possible searching locations are limited into a set of finite RP locations. Therefore, the performance of such fingerprint-based localization is constrained by the RP granularity. In general, a finer RP granularity provides more detailed description of radio propagation characteristics, and often leads to a higher localization accuracy. However, a finer RP granularity means that more RPs per unit area should be measured in the offline phase, which introduces prohibitive costs of time and labor in turn.

To relieve the training burden, some previous work [8–11] suggest exploiting unlabeled data, such as measurements of user casual movement traces, to improve the calibration of RSS distributions. In [8,9,11], the EM algorithm is used to improve the fingerprint distributions based on a small fraction of training reference points and the collection of user traces. In [10], the relative locations of access points and mobile targets are first determined by using some unlabeled data in the offline phase. In the online phase, their absolute locations are recovered to help locating a target for a given set of labeled data. Generally, these approaches help to reduce the fingerprint calibration efforts, but they are still a kind of discrete scheme with limited fingerprints.

Some work suggest enriching the reference points by creating virtual reference points and interpolating their fingerprints based on the spatial correlation of radio propagation. The interpolation can be done either in the offline phase [7,11,12] or in the online phase [17]. However, both of the two methods need a large storage space to store the fingerprints. The online interpolation is also very time-consuming, because one should first select several candidate RPs during the online phase and then conduct interpolation in the area surrounded by these RPs. Our proposed surface fitting method could save the storage space efficiently, as only a few of fitting function coefficients need to be saved. Furthermore, it has been shown in our simulations and experiments that the proposed GLS method can obtain the positioning location only by a few iterations.

To reduce the online fingerprint comparisons, fingerprint clustering methods have been proposed to group fingerprints into some clusters [18–21]. In the online phase, a mobile is first determined to which cluster it belongs, and then comparisons

Please cite this article in press as: B. Wang, et al., Indoor positioning via subarea fingerprinting and surface fitting with received signal strength, Pervasive and Mobile Computing (2015), http://dx.doi.org/10.1016/j.pmcj.2015.06.011

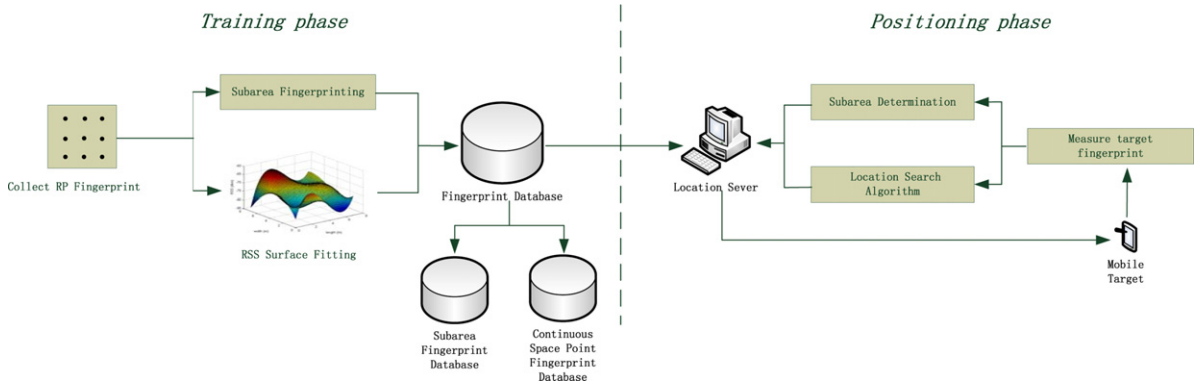

Fig. 1. The schematic diagram of the proposed subarea-based localization system.

are only made to those fingerprints within the selected cluster. All these clustering methods are conducted in the signal space, and the RPs in a cluster often form an irregular subarea. In our work, we exploit the indoor layout, such as partitions and rooms, to divide reference points into subareas. By using such a subarea division and determination scheme, more accurate RSS distribution fitting functions can be obtained in subarea levels. Furthermore, a coarse yet meaningful subarea location service can be provided for some applications with less demanding location requirements.

3. Offline subarea fingerprinting and RSS surface fitting

3.1. Preliminaries

The traditional fingerprint localization process can be generally divided into two phases: the offline training phase and online positioning phase. In the offline phase, a fingerprint database is established as follows. For a given indoor environment, suppose that there are M APs, and N evenly-distributed RPs $l_i, i = 1, 2, \ldots, N$, each with known coordinate. At each RP l_i, we measure the RSS from M APs for a period of time and generate an averaged RSS vector as its fingerprint $\mathbf{s}_i \doteq (s_{i1}, s_{i2}, \ldots, s_{iM})$, where s_{ij} denotes the average RSS from the jth AP at l_i. If the jth AP cannot be detected, we simply set a very small value for s_{ij}, say for example, $s_{ij} = -100$ dB. All the fingerprints are stored in a database.

In the online positioning phase, a mobile target compares its real-time fingerprint $\mathbf{s}^o \doteq (s_1^o, s_2^o, \ldots, s_M^o)$ with those prestored in the fingerprint database, and estimates its location by some localization algorithm. Take the nearest neighbor in signal space algorithm (NN) as an example. The estimated location $\hat{l}$ is given by

$$\hat{l} = \arg\min_{l_i} \sum_{j=1}^{M} (s_{ij} - s_j^o)^2, \quad i = 1, 2, \ldots, N. \tag{1}$$

In indoor environments, concrete walls introduce a significant attenuation effect on radio transmission, which often causes several dB path loss in the received signal strength. On the other hand, space points that are close in the Euclidean space often experience similar received signal strengths due to the spatial correlation of radio propagation [22]. These have been collaborated by our field experiments. Fig. 2 plots the measured RSSs from AP 1 of three selected RPs. The details of our field experiments are introduced in Section 5. In particular, we select RP a and RP b in room 301 and RP c in room 303, as represented by circles in Fig. 4. It is observed that the two RPs in room 301 experience similar RSSs, and the difference of their mean RSSs is about 1 dB. It is also observed that the mean RSS difference of RPs in different rooms is about 6 dB, which is mainly caused by concrete wall attenuation. These observations have motivated us to design a subarea-based indoor localization scheme. In this paper, we use some natural building partitions to obtain subareas, such as rooms.

Fig. 1 plots the schematic diagram of the proposed scheme. In the offline phase, we first establish a subarea fingerprint database, and then apply the surface fitting technique to obtain space point RSS fitting functions. The online positioning phase is divided into two steps. In the first step, we determine to which subarea the measured fingerprint belongs, and in the second step, we apply a location search algorithm to estimate its location within the subarea. The details of the proposed scheme are presented in this and next section.

3.2. Subarea fingerprinting

The subarea fingerprint database is constructed based on the fingerprints of RPs. Assume that the given indoor environment can be divided into K subareas. All RPs in the kth subarea are grouped into a RP set $\mathcal{R}_k$, $k = 1, 2, \ldots, K$. We create a subarea fingerprint $F_k = (S_{k1}, S_{k2}, \ldots, S_{kM})$ for each subarea, where S_{kj} denotes the average received signal strength from

Please cite this article in press as: B. Wang, et al., Indoor positioning via subarea fingerprinting and surface fitting with received signal strength, Pervasive and Mobile Computing (2015), http://dx.doi.org/10.1016/j.pmcj.2015.06.011

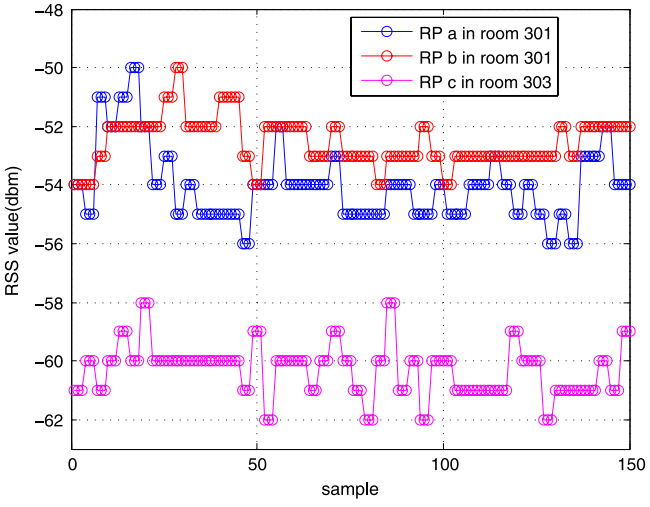

Fig. 2. Measured RSSs of the three selected RPs in our field experiments.

the jth AP in the kth subarea. Since RPs in the same subarea often suffer similar signal propagation while their fingerprints differ significantly if they were distributed in different subareas, then S_{kj} can be simply obtained as follows:

$$S_{kj} \doteq \frac{1}{|\mathcal{R}_k|}\sum_{i=1}^{|\mathcal{R}_k|} s_{ij}, \quad i \in \mathcal{R}_k,\ j = 1, \ldots, M. \tag{2}$$

3.3. RSS surface fitting

The surface fitting is a well known technique to construct a continuous function from a finite set of discrete data [23]. The advantage of this technique is that it takes into consideration of the data change trend in the function construction. In this paper, we apply the surface fitting to construct the RSS distribution function in each subarea based on the RPs' fingerprints for every AP. We build M continuous functions for one subarea and $M \times K$ functions for the whole area. We then can establish the fingerprint of an arbitrary space point based on these functions.

Let $\phi_{kj}(x, y)$ denote the fitted RSS distribution function for the kth subarea and the jth AP, where (x, y) is the coordinate of a space point within the kth subarea. Let (x_i, y_i) denote the coordinate of the ith RP in the kth subarea, and s_i its average RSS from the jth AP. Suppose that there are n RPs in the kth subarea. The objective of constructing an RSS fitting function is to minimize the following sum of squared error based on the least square (LS) principle:

$$\text{minimize} \quad h \equiv \sum_{i=1}^{n}(\phi_{kj}(x_i, y_i) - s_i)^2. \tag{3}$$

The adoption of the LS principle is because the fitting function is asked to nearly across all the fitting data so that the RSS spatial distribution can be well reflected in the fitted function. For ease of presentation, we next omit the subscription for $\phi(x, y)$.

Multivariate polynomial functions have been widely adopted to construct fitting functions in many fields due to its simplicity and effectiveness [24,25]. In this paper, we use binary polynomial functions to construct $\phi(x, y)$ as follows:

$$\phi(x, y) = \sum_{c=1}^{p}\sum_{d=1}^{q} a_{cd}x^{c-1}y^{d-1}. \tag{4}$$

If we introduce vectors $\mathbf{x} = [1\ x\ x^2\ \cdots\ x^{p-1}]^{tr}$, $\mathbf{y} = [1\ y\ y^2\ \cdots\ y^{q-1}]^{tr}$, and matrix

$$\mathbf{A} = \begin{bmatrix} a_{11} & a_{12} & \cdots & a_{1q} \\ a_{21} & a_{22} & \cdots & a_{2q} \\ \vdots & \vdots & \ddots & \vdots \\ a_{p1} & a_{p2} & \cdots & a_{pq} \end{bmatrix}. \tag{5}$$

Then Eq. (4) can be written conveniently in a matrix format as $\phi(x, y) = \mathbf{x}^T\mathbf{A}\mathbf{y}$. Note that the sum of squared error h is a quadratic function about variables a_{cd}, and $a_{cd} = \{a_{11}, \ldots, a_{er}, \ldots, a_{pq}\}$, $e = 1, \ldots, p$, $r = 1, \ldots, q$.

Please cite this article in press as: B. Wang, et al., Indoor positioning via subarea fingerprinting and surface fitting with received signal strength, Pervasive and Mobile Computing (2015), http://dx.doi.org/10.1016/j.pmcj.2015.06.011

To minimize h, we equate its partial derivatives to zero with respect to each variable a_{er}.

$$\begin{aligned}\frac{\partial h}{\partial a_{er}} &= \frac{\partial}{\partial a_{er}}\sum_{i=1}^{n}[\phi(x_i, y_i) - s_i]^2 \\ &= \sum_{i=1}^{n}\left\{2[\phi(x_i, y_i) - s_i]\frac{\partial}{\partial a_{er}}[\phi(x_i, y_i)]\right\} \\ &= \sum_{i=1}^{n}\{2[\phi(x_i, y_i) - s_i]x_i^{e-1}y_i^{r-1}\} \\ &= 0. \end{aligned} \tag{6}$$

From the above equation we can derive

$$\sum_{i=1}^{n} x_i^{e-1}y_i^{r-1}\phi(x_i, y_i) = \sum_{i=1}^{n} x_i^{e-1}y_i^{r-1}s_i, \tag{7}$$

$$\sum_{i=1}^{n} x_i^{e-1}y_i^{r-1}\sum_{c=1}^{p}\sum_{d=1}^{q} a_{cd}x_i^{c-1}y_i^{d-1} = \sum_{i=1}^{n} x_i^{e-1}y_i^{r-1}s_i. \tag{8}$$

For the computation convenience, we rewrite the above equation as:

$$\sum_{c=1}^{p}\sum_{d=1}^{q}\left[a_{cd}\sum_{i=1}^{n}(x_i^{e-1}y_i^{r-1}x_i^{c-1}y_i^{d-1})\right] = \sum_{i=1}^{n} x_i^{e-1}y_i^{r-1}s_i \tag{9}$$

and introduce expression $u_{cd}(e, r)$ and $v(e, r)$, where

$$u_{cd}(e, r) = \sum_{i=1}^{n}(x_i^{c-1}y_i^{d-1}x_i^{e-1}y_i^{r-1}),$$

$$v(e, r) = \sum_{i=1}^{n} x_i^{e-1}y_i^{r-1}s_i,$$

then Eq. (8) can be written as:

$$\sum_{c=1}^{p}\sum_{d=1}^{q} a_{cd}u_{cd}(e, r) = v(e, r), \quad e = 1, \ldots, p,\ r = 1, \ldots, q. \tag{10}$$

In fact, the above formula has w equations, $w = p \times q$. Convert it into a matrix form as $\mathbf{Ua} = \mathbf{V}$.

$$\underbrace{\begin{bmatrix} u_{11}(1, 1) & \cdots & u_{pq}(1, 1) \\ \vdots & \ddots & \vdots \\ u_{11}(p, q) & \cdots & u_{pq}(p, q) \end{bmatrix}}_{U}\underbrace{\begin{bmatrix} a_{11} \\ \vdots \\ a_{pq} \end{bmatrix}}_{a} = \underbrace{\begin{bmatrix} v(1, 1) \\ \vdots \\ v(p, q) \end{bmatrix}}_{V}. \tag{11}$$

Then $\mathbf{a} = \mathbf{U}^{-1}\mathbf{V}$. Here $\mathbf{a}$ is a $w \times 1$ matrix, and we need to convert it into a $p \times q$ matrix $\mathbf{A}$. For any location (x, y) in the subarea, the RSS at this point can be computed by $s = \phi(x, y) = \mathbf{x}^T\mathbf{Ay}$.

We next present an example of fitting function based on field measured data. For Room 301, we apply all the 25 RPs to conduct surface fitting for AP 3. Figs. 3(a) and (b) plot the fitted surface with $(p, q) = (2, 2)$ and $(p, q) = (5, 5)$, respectively. The surface fitting function equation with $(p, q) = (2, 2)$ is as follows:

$$\phi(x, y) = -74.2542 + 0.8110 \times y - 0.2491 \times x + 0.0323 \times xy.$$

We omit the equation for $(p, q) = (5, 5)$ due to its long expression. Fig. 3(c) plots the measured and fitted RSS for the 25 RPs. It can be observed that using $(p, q) = (5, 5)$ has a smaller fitting error and could provide a better description of the signal propagation characteristics; Yet using a large (p, q) brings many peaks and valleys in the fitted surface as shown in Fig. 3(b), and may introduce the overfitting problem when the number of RPs used for surface fitting is not enough. On the other hand, although using $(p, q) = (2, 2)$ may produce a larger fitting error, it still can reflect the basic signal change trend as shown in Fig. 3(a). What is more, using a small (p, q) only requires a few of RPs for the fitting, which can greatly reduce field measurements.

4. Online subarea determination and location search

The online positioning phase consists of two steps: subarea determination and location search.

Please cite this article in press as: B. Wang, et al., Indoor positioning via subarea fingerprinting and surface fitting with received signal strength, Pervasive and Mobile Computing (2015), http://dx.doi.org/10.1016/j.pmcj.2015.06.011

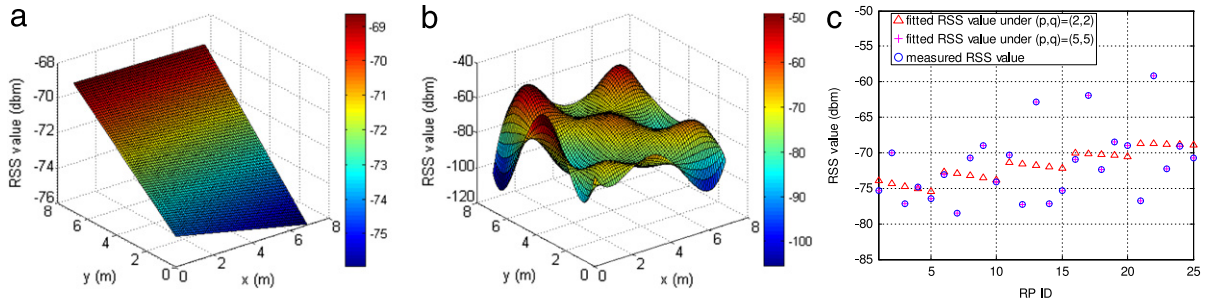

Fig. 3. (a) Fitted surface with $(p, q) = (2, 2)$; (b) Fitted surface with $(p, q) = (5, 5)$; (c) Comparison of fitted RSS and measured RSS under different (p, q) choices.

4.1. Subarea determination

The subarea determination is based on the nearest neighbor in signal space. The localization server compares the mobile fingerprint $\mathbf{s}^o \doteq (s_1^o, \ldots, s_M^o)$ with subarea fingerprints F_k, $k = 1, 2, \ldots, K$, and the subarea with the minimum fingerprint difference is selected. For the kth subarea, the fingerprint difference is computed by

$$D_k \doteq \|F_k - \mathbf{s}^o\| = \sqrt{\sum_{j=1}^{M}(S_{ij} - s_j^o)^2}. \tag{12}$$

The subarea with the minimum D_k is selected.

4.2. Location search

Suppose that the kth subarea is selected in the first stage. In the second step, we search a space point $(\hat{x}, \hat{y})$ within the selected subarea, such that the signal space difference between its fingerprint and $\mathbf{s}^o$ is minimized. That is,

$$(\hat{x}, \hat{y}) = \arg\min_{(x,y)} J \equiv \sum_{j=1}^{M}(\phi_{kj}(x, y) - s_j^o)^2. \tag{13}$$

In this paper, we propose two methods to conduct location search: exhaustive search and gradient descent search.

4.2.1. Exhaustive search

In the exhaustive search, we use a grid lattice to represent the subarea. For a grid point with coordinate (x, y), its fingerprint can be computed by the RSS fitting functions $\phi_{k1}(x, y), \phi_{k2}(x, y), \ldots, \phi_{kM}(x, y)$. Then traverse every grid point and find a point which could satisfy the objective function (13). Obviously, this method is of high computation complexity, if the grid step size is small. On the other hand, a smaller step size may help to improve the accuracy of location search, as the space is described finely. In this paper, we choose a step size of 0.1 m for a typical office scenario.

4.2.2. Gradient descent search

This method is to iteratively search a location $l \equiv (x, y)$ to reduce $J(l)$ in each iteration. Let $l^{(t)}$ denote the location in the tth iteration, $t = 0, 1, 2, \ldots$. The search iteration is defined by

$$l^{(t+1)} = l^{(t)} + \alpha^{(t)} \times d^{(t)} \tag{14}$$

where $\alpha^{(t)}$ is the search step and $d^{(t)}$ is the search direction, respectively. Generally, the search step can be a constant or an adjustable value. To achieve a better performance, in this paper, we allow an adjustable search step.

Determine $l^{(0)}$: $l^{(0)}$ is the initial location of the iterative search process. Generally, it can be randomly selected. However, a random one may lead to numerous iterations and even fall into a local minima in some cases. To improve the search efficiency, in this paper we set the initial point as the NN localization result in the target subarea (this localization scheme is also called SD-NN method which will be introduced in Section 5).

Determine $d^{(t)}$: For the function $J(l^t)$, the gradient at the location $l^{(t)}$ is computed by

$$\nabla J(l^{(t)}) = \left[\frac{\partial J(l^{(t)})}{\partial x}, \frac{\partial J(l^{(t)})}{\partial y}\right]^{tr},$$

and its direction is the fastest growth direction of $J(l^{(t)})$. Therefore, to reach the minimum point of $J(l)$ quickly, the negative gradient direction is used as the search direction. That is, $d^{(t)} = -\nabla J(l^{(t)})$.

Please cite this article in press as: B. Wang, et al., Indoor positioning via subarea fingerprinting and surface fitting with received signal strength, Pervasive and Mobile Computing (2015), http://dx.doi.org/10.1016/j.pmcj.2015.06.011

Table 1
Gradient descent search algorithm.

Gradient descent search:
Input: J, d_{min}, t_{max}
Output: $\hat{l}(x, y)$, the estimated target location

```
1:  t = 0
2:  Get the initial location l^(0)
3:  while (t < t_max)
4:    Compute the gradient ∇J(l^(t));
5:    Compute the search step α^(t);
6:    Compute the new location l^(t+1);
7:    if l^(t+1) is outside of the subarea
8:      l^(t+1) = l^(t);
9:      break;
10:   if ||l^(t+1) − l^(t)|| < d_min
11:     break;
12:   t = t + 1;
13:   Goto 3;
14: endwhile
15: return l^(t+1)
```

Determine $\alpha^{(t)}$: Given the search direction $d^{(t)}$ in the tth iteration, then in the $(t+1)$th iteration, $J(l^{(t+1)})$ becomes a function of $\alpha^{(t)}$. We adopt the Golden Section method to obtain $\alpha^{(t)}$, which satisfies

$$\alpha^{(t)} = \arg\min_{\alpha} J(l^{(t)} - \alpha \nabla J(l^{(t)})). \tag{15}$$

The Golden Section method is a classical one-dimensional optimization method [26]. It works as follows: insert two points a_1, a_2 in the search interval $[t_1, t_2]$, so the interval is divided into three sections $[t_1, a_1]$, $[a_1, a_2]$, $[a_2, t_2]$. Here

$$\begin{aligned} a_1 &= t_2 - 0.618 * (t_2 - t_1); \\ a_2 &= t_1 + 0.618 * (t_2 - t_1). \end{aligned} \tag{16}$$

In this paper, we set the original search interval $[t_1, t_2]$ as $[0, 0.5]$. We first compare the value of $J(a_1)$ and $J(a_2)$, and reset the search interval as $[t_1, a_2]$ if $J(a_1) < J(a_2)$, or then choose search interval $[a_1, t_2]$. Repeat above procedure in the new generated interval until $\|t_2 - t_1\|$ is smaller than a threshold e_{min}. In our simulations and experiments, we set $e_{min} = 0.01$ for the accuracy consideration. Finally, $(t_2 + t_1)/2$ is used as the search step $\alpha^{(t)}$.

Terminate conditions: We set three termination conditions for the gradient descent search, and the process will be terminated if any one of the them is satisfied.

(1) If the iterative times exceed a threshold t_{max}, the iteration terminates. This is because the convergence rate drops rapidly when the iterative times becomes large. We want to terminate the iteration in limited steps. In this paper we set t_{max} equal to 10.
(2) If the Euclidean distance of two successive search locations $\|l^{(t+1)} - l^{(t)}\|$ is smaller than a predefined threshold d_{min}, the iteration terminates. To make a fair comparison with the exhaustive search method, in this paper we set d_{min} equal 0.1 m.
(3) If $l^{(t+1)}$ is outside of the target subarea, then the last iterative location $l^{(t)}$ is chosen as the estimate location.

Complete steps of gradient descent search are given in Table 1.

5. Simulation and experiment results

5.1. Simulation and experiment environment

We conduct simulations and experiments for a typical office scenario, the third floor of the Next Generation of the Internet Access System State Engineering Laboratory in our university, which includes eight office rooms and one corridor. The total floor layout is of 16.2 m × 28.5 m large, and each room is of 6.8 m length and 6.9 m width. The thickness of one wall is 0.3 m. Fig. 4 plots the floor layouts, where a 2D coordinate system is used to describe the location of one point and the origin point is chosen as the left-upper corner point of room 301. In our simulations and experiments, we deployed 8 APs totally. The reference points are created according to the normal fingerprint technique by a grid approach. There are 25 evenly-distributed RPs per room, each separated by 1.6 m both horizontally and vertically.

We compare our proposed algorithms with the traditional fingerprint-based nearest neighbor algorithm with the subarea determination scheme (denoted as SD-NN). In SD-NN, we first locate a mobile into a subarea and then conduct the nearest neighbor algorithm in the selected subarea. For the ease of presentation, our proposed algorithm is denoted as SF-ELS (surface fitting and exhaustive location search) algorithm and SF-GLS (surface fitting and gradient descent location search) algorithm, respectively.

Please cite this article in press as: B. Wang, et al., Indoor positioning via subarea fingerprinting and surface fitting with received signal strength, Pervasive and Mobile Computing (2015), http://dx.doi.org/10.1016/j.pmcj.2015.06.011

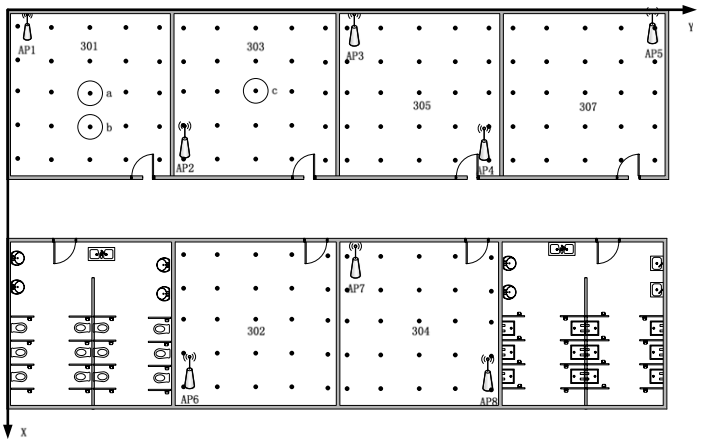

Fig. 4. Third floor of the Next Generation of the Internet Access System State Engineering Laboratory. The dots represent the RP locations.

Table 2
Hit rate performance study.

L_w (dB)[a]	0	1	2	3	4	5
Hit rate	94.2%	98.5%	99.2%	99.8%	100%	100%
AP number[b]	4	5	6	7	8	
Hit rate	99.8%	100%	100%	100%	100%	
RP per room[c]	6	10	15	20	25	
Hit rate	100%	100%	100%	100%	100%	

[a] 8 APs and 25 RPs per room are used.
[b] $L_w = 3$ dB, and 25 RPs per room are used.
[c] $L_w = 3$ dB, and 8 APs are used.

5.2. Simulation results

In our simulations, we apply the Keenan–Motley model [27] to describe the indoor radio propagation characteristics. It takes multipath fading and the attenuation effect of obstructions in the propagation route into account, and is given by

$$PL(d) = PL_c - 10\beta \log \frac{d}{d_0} + \sum_{i=1}^{I} N_{wi} L_{wi} + X(\sigma) \tag{17}$$

where PL_c is the signal transmission power of the signal source, β is the environment attenuation coefficient, d_0 the reference distance, N_{wi} the number of ith type walls between the AP and the receiver, L_{wi} the corresponding wall loss factor, I the total number of walls, and $X(\sigma)$ is a zero-mean Gaussian random variable with a standard deviation σ. In addition, we set parameter $PL_c = 37.3$ dB, $d_0 = 1$ m, $n = 2$, and $\sigma = 3$ dB, respectively. In our simulations, the main obstacles are concrete walls. We set 5 dB for the attenuation value L_w caused by one wall, which was calibrated from our field experiment.

We randomly select 200 test points in the environment to verify the performance of our proposed method. The localization metric is the *average localization error*, which is defined as the Euclidean distance difference between the estimated location and the real location averaged over all the test points.

5.2.1. Subarea determination performance

We first examine the subarea hit rate performance. The hit rate is defined as the ratio between the number of the correct subarea determination to the total number of tests. Table 2 records the hit rate against different parameter values, including wall attenuation L_w, AP number (using 25 RPs per room), and RP number used per room (using 8 APs). It is easy to find that the wall attenuation really helps to improve the hit rate performance. The larger the value of L_w, the higher the hit rate. This is not unexpected, as the subarea division based on rooms by the surrounding concrete walls provides a high fingerprint discrimination. Furthermore, it is also shown that our subarea determination method can achieve very high hit rate, close to 1, even fewer APs and RPs are used for subarea fingerprinting.

5.2.2. Localization error vs. fitting parameter

When constructing a fitting function, the larger the value of (p, q), the more the coefficients and the higher the computation complexity. We vary them from $(2, 2)$ to $(5, 5)$ in our simulations to examine how they impact the localization performance.

Please cite this article in press as: B. Wang, et al., Indoor positioning via subarea fingerprinting and surface fitting with received signal strength, Pervasive and Mobile Computing (2015), http://dx.doi.org/10.1016/j.pmcj.2015.06.011

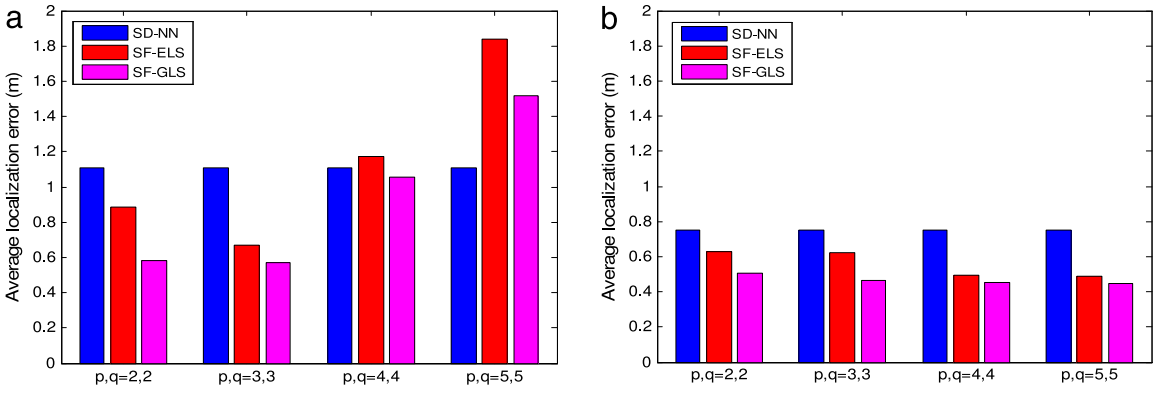

Fig. 5. Comparison of localization error under different values of (p, q) when (a) 15 PRs are used per room, (b) 25 RPs are used per room.

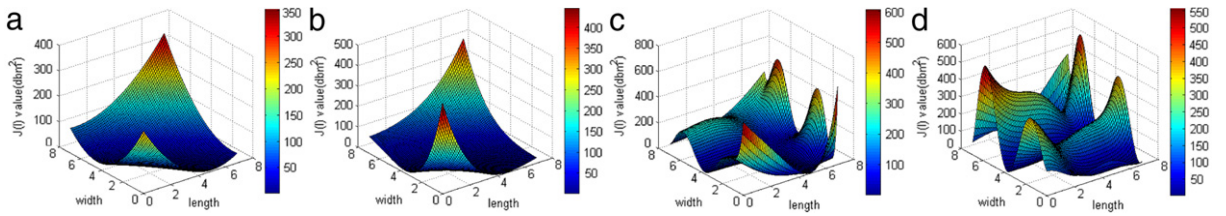

Fig. 6. An illustration of the objective function $J(l)$ value when using 15 RPs per room under (a) $(p, q) = (2, 2)$, (b) $(p, q) = (3, 3)$, (c) $(p, q) = (4, 4)$, and (d) $(p, q) = (5, 5)$.

Figs. 5(a) and (b) compare the localization performance of the three algorithms, when using 15 RPs per room and 25 RPs per room (using 8APs), respectively, for fitting functions. It is first observed that both SF-ELS and SF-GLS perform better than SD-NN in terms of smaller localization errors. This is because through surface fitting we construct a continuous fingerprint distribution function, which introduces a finer description of radio propagation characteristics and enriches the search space during the localization phase. We next observe that the SF-GLS has an improvement compared to the SF-ELS. This is caused by two reasons: First, in our simulations we set the exhaustive search grid resolution 0.1 m, while for the gradient descent search we use an adjustable search step which may be smaller than 0.1 m in some cases. That is, the SF-GLS is conducted in a larger search space. Second, for the gradient descent search, it is based on the slope information provided by the objective function. So as long as the surface could describe the change trend of the signal correctly, then we can reach an approximate optimizer in the negative gradient direction. For the exhaustive search, the target location is determined by the accuracy of fitted RSSs. If the fitted RSS surface is not very accurate, a small fluctuation of the RSS fitting surface may cause a large localization deviation.

We next study how does (p, q) value affect the localization performance. Fig. 5 compares the localization performance when 15 and 25 RPs are used per room with difference choices of (p, q). First, we observe that increasing (p, q) does not always improve the localization accuracy. It is also dependent on the RP number used per room. If sufficient RPs are used, a large (p, q) means that the fitting function can describe the RSS distribution more accurately and leads to a better localization accuracy, as observed from Fig. 5(b).

On the other hand, if fewer RPs are used for surface fitting, the localization performance degrades much when using a large (p, q) like (5, 5), as observed from Fig. 5(a) with only 15 RPs. This is due to the so-called *over-fitting* problem. For fewer RPs and larger (p, q), there may appear many peaks and valleys in the fitted surface, which makes the fitting function inaccurate and further causes an unsmooth objective function $J(l)$, as shown in Fig. 6(c) and (d). Second, it can be also found that a smaller (p, q), like (2, 2) and (3, 3), does not cause great performance degradation, especially for the SF-GLS method. This is because a smaller (p, q) contributes to a smooth function $J(l)$, as shown in Fig. 6(a) and (b). Usually, a function with smooth surface is conducive to the gradient descent method. Furthermore, a larger (p, q) often leads to prohibitive computation costs during the online positioning phase. To balance the localization accuracy and the computation cost, we suggest setting $(p, q) = (2, 2)$ in this paper.

5.2.3. Localization error vs. RP granularity

Fig. 7 plots the localization error against different RP numbers per room from 6 to 25. It is easy to find that all the three algorithms benefit from a finer RP granularity (more RPs per room), because the radio propagation distribution can be better described when more measured fingerprints are used. However, both SF-ELS and SF-GLS are less sensitive to the RP granularity than SD-NN. Recall that the NN positioning algorithm locates a mobile to one RP with the smallest signal space difference. The localization accuracy is constrained by the RP granularity. Therefore, the NN positioning performance will be

Please cite this article in press as: B. Wang, et al., Indoor positioning via subarea fingerprinting and surface fitting with received signal strength, Pervasive and Mobile Computing (2015), http://dx.doi.org/10.1016/j.pmcj.2015.06.011

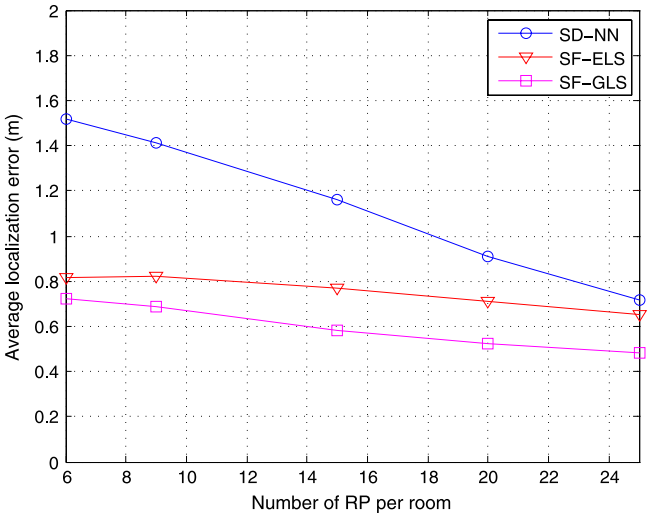

Fig. 7. Localization error vs. the number of used RP per room.

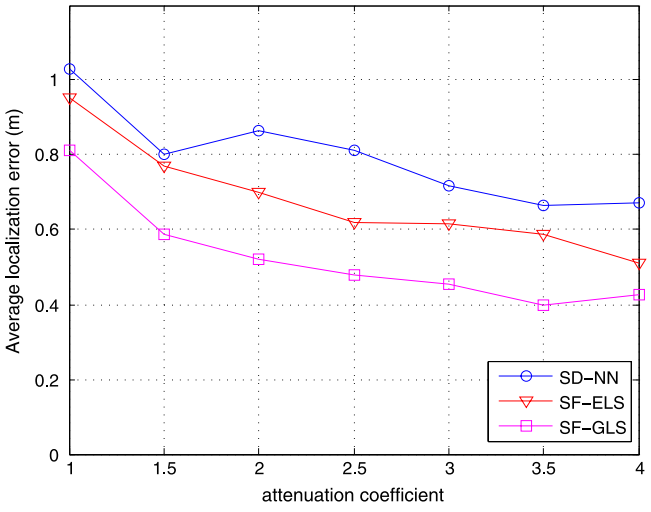

Fig. 8. Comparison of localization error under different environment attenuation value.

improved when more RPs put into used. On the other hand, the surface fitting method takes the radio propagation correlation into consideration to reconstruct a continuous RSS distribution function, and may only need a few of RPs per room for the reconstruction. This is a good news. Since the offline RP training process is quite time-consuming and labor-intensive, our method can help to cut costs and is more practical for large environments.

5.2.4. Localization error vs. propagation parameter

Fig. 8 plots the localization error vs. the attenuation coefficient β. It is seen that all algorithms benefit from a larger attenuation coefficient. This is because when β increases, the path loss also becomes large, which helps to increase the RP fingerprint discrimination more effectively. Fig. 9 plots the localization error against the propagation parameter σ from 0 dB to 5 dB. It is shown that all the three algorithms suffer from higher variation of the propagation shadowing, but the SF-GLS still performs the best even in a harsh environment.

5.3. Experimental results

We have conducted two batches of field experiments to test the proposed algorithms in winter and summer (January and August of 2013), respectively. Channel measurements of a WLAN at 2.4 GHz based on 802.11 g standard were conducted for RSS samplings. The TP-Link TL-WR740N® wireless routers were used as APs. In our experiments, we simply plugged in these routers to collect RSS samplings by using all default configurations of these off-the-shelf routers. The AP placement in the first batch is as plotted in Fig. 4, but the AP placement in the second batch is a little bit different, because the furniture

Please cite this article in press as: B. Wang, et al., Indoor positioning via subarea fingerprinting and surface fitting with received signal strength, Pervasive and Mobile Computing (2015), http://dx.doi.org/10.1016/j.pmcj.2015.06.011

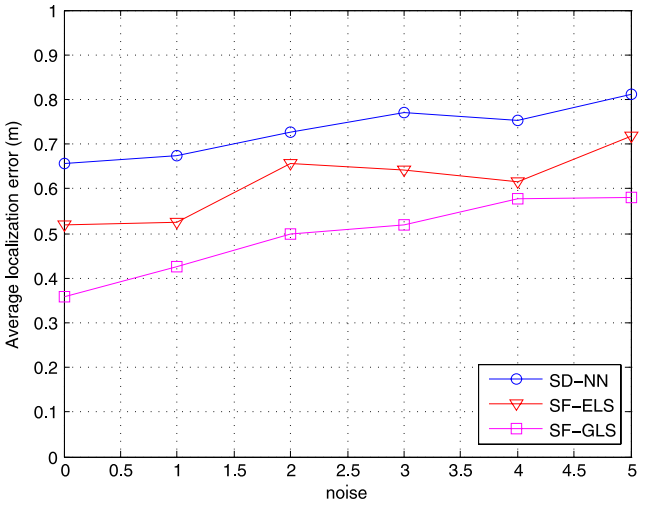

Fig. 9. Comparison of localization error under different noise level.

Fig. 10. A part of the test office room. A tripod was used to hold a mobile phone for RSS samplings in the summer batch.

layout was changed a little half a year later. In particular, only the 2th and 5th AP locations are shifted no more than 1.0 m away from the first batch.

Fig. 10 pictured a part of office layout and our measurement in summer. Here we use a tripod to support a mobile in the summer batch; while a mobile device is held by a person in the winter batch. Note that in the two experiment batches, we did not control the people movement in each office room, and the flow of people was actually changing with time. Generally, during the office time, more people walked around and in/out the room. During the lunch time, only our testers and on-duty staffs stayed in the room. In addition, the flow of people in summer was larger than in winter, because more people walked around during the experiment. In a short summary, our testing conditions were the same as everyday life in order to test our algorithms in realistic scenarios.

In each experiment batch, we conduct extensive field measurements to collect RSS samples for both reference points and testing points. The RSS sampling rate is set as 2 samples per second, and each reference point is with 150 samples and each testing point is with 20 samples. In the first batch, a Xiaomi 1S® mobile phone with Android 4.0 operating system was used for RSS sampling and positioning. In the second batch, besides using a Xiaomi 1S®, a Huawei U8860® mobile phone with Android 2.3 operating system was also used for positioning. The reason of using two kinds of mobile devices is to cross-test the proposed algorithms in different hardware platforms.

5.3.1. Subarea determination performance

Table 3 presents the subarea hit rate performance against the number of RPs per room (using 8 APs) and the number of AP (using 25 RPs per room). It is observed that the average hit rate is above 92% under different conditions. So exploiting the natural division of the concrete walls to increase the fingerprint discrimination and making subarea determination are feasible in practical indoor environments.

Please cite this article in press as: B. Wang, et al., Indoor positioning via subarea fingerprinting and surface fitting with received signal strength, Pervasive and Mobile Computing (2015), http://dx.doi.org/10.1016/j.pmcj.2015.06.011

Table 3
Hit rate performance study.

RP per room[a]	6	10	15	20	25
Hit rate	94.87%	92.31%	93.59%	92.31%	93.59%
AP number[b]	4	5	6	7	8
Hit rate	92.31%	91.03%	94.87%	96.15%	93.59%

[a] 8 APs are used.
[b] 25 RPs per room are used.

Table 4
The APs used in the localization.

AP number	AP index	AP number	AP index
4	2,3,4,7	5	2,3,4,6,8
6	2,3,4,6,7,8	7	1,2,3,4,5,6,7

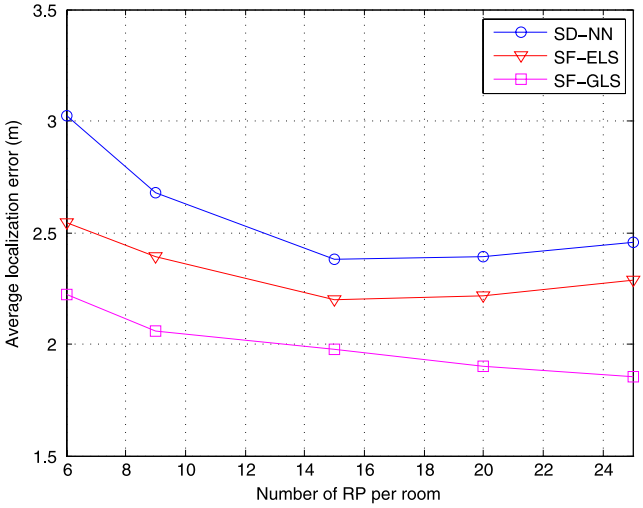

Fig. 11. Experiment results: localization error vs. the number of used RP per room.

5.3.2. Localization performance study

Fig. 11 plots the localization error against the number of RPs per room (using 8 APs) based on the winter experiment batch. It is observed that all the three algorithms performance improve, when more training RPs are used. Both the two proposed methods perform better than SD-NN, and the SF-GLS performs best. In particular, the average improvement of SF-ELS and SF-GLS compared with the SD-NN algorithm are about 10% and 22%, respectively. What is more, the performance of SF-GLS when using only 6 RPs per room is still better than the SD-NN method when using 25 RPs per room (2.22 m against 2.46 m). In other words, our proposed SF-GLS method could achieve 10% accuracy improvement while reduce 76% workload compared with the traditional fingerprint method in this case. This is because using the surface fitting for RSS distribution construction provides a finer description for radio propagation characteristics and also enriches the location search space. These are consistent with our previous simulation results. Note that due to the complex indoor environment and the limited RSS sensitivity of the mobile device (the signal strengths are quantized into discrete levels by the device [28]), the minimum localization error is 1.85 m in our field experiments, which is worse than that in simulation results.

Fig. 12 tests the localization performance when different numbers of APs are used based on the winter experiment batch. The AP selection is listed in Table 4. It is first observed that the proposed SF-GLS algorithm achieves the lowest localization errors among the three algorithms. Furthermore, with the increase of the number of used APs, the localization errors of the three algorithm decrease. The reason is that using more APs helps to increase the RSS fingerprint discrimination in between different RPs. Note that using the less AP number is time-saving and requires less computation.

5.3.3. Localization error vs. different devices

We next evaluate the proposed algorithms considering device heterogeneity. That is, the RPs are sampled by Xiaomi 1S and test points are sampled and positioned by both Xiaomi 1S and Huawei U8860. In general, different types of device often observe different RSS values due to the hardware difference. Fig. 13 plots the RSS samplings at the same place using different devices. It can be seen that the average observed RSS value by Huawei U8860 is larger than that by Xiaomi 1S. In addition, the former device is more steady than the latter.

Please cite this article in press as: B. Wang, et al., Indoor positioning via subarea fingerprinting and surface fitting with received signal strength, Pervasive and Mobile Computing (2015), http://dx.doi.org/10.1016/j.pmcj.2015.06.011

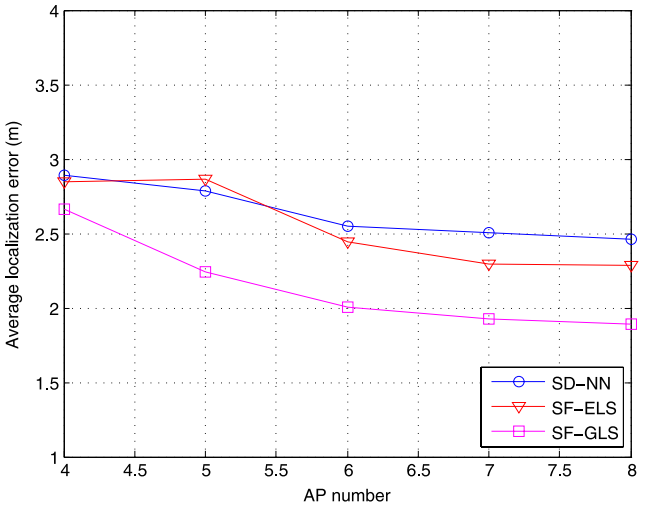

Fig. 12. Experiment results: localization error vs. the number of used AP.

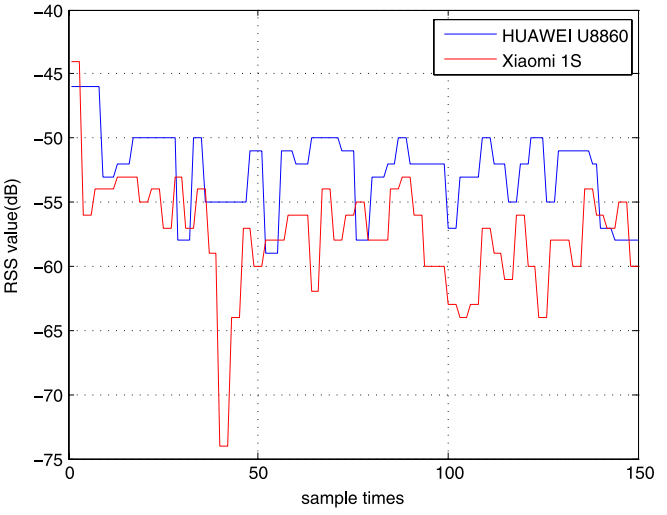

Fig. 13. Comparison of RSS samplings at the same place using two types of devices at the same time. The mean and standard deviation of RSS values for Huawei U8860 are −52.6 dB and 3.1 dB, respectively, and for Xiaomi 1S, are −57.5 dB and 4.3 dB, respectively.

Fig. 14 compares the localization performance based on our summer experiment batch. First, we can observe that the proposed SF-GLS method performs better than traditional fingerprint method, even using different devices. The localization accuracy improvement of our proposed method against SD-NN method is remarkable. In detail, the median error of SF-GLS and SD-NN for Xiaomi 1S is 2.79 m and 3.26 m, and for Huawei U8860 is 2.05 m and 2.86 m, respectively. Second, it is found that the Huawei U8860 device performs better than the Xiaomi 1S. This is because that the Huawei device is more steady for RSS sampling which was observed from Fig. 13.

5.3.4. Localization error vs. environment condition change

In practice, the signal propagation environment is always changing, which may result in RSS fluctuations. The ability of environmental change tolerance is one of the important performance indices for a RSS-based indoor localization system. Because the offline RP training phase and the online target positioning phase are often conducted in different days or months in practice. In this section, we evaluate the robustness performance of our proposed algorithm when the environment conditions change. As mentioned before, our two experiment batches are separated almost half a year, and one was in winter and another in summer. Here we use the RPs' RSS values sampled in winter for fingerprinting and surface fitting, and test points sampled in summer by Xiaomi 1S are used for positioning.

From Fig. 15, we can see that the SF-GLS is less sensitive to the environmental change than the traditional fingerprinting-based method. In Fig. 15, the RPs are sampled in winter, but for the SF-GLS algorithm, its localization performance of using summer samples of testing points is not much degraded than that using winter samples. Furthermore, when using RPs and

Please cite this article in press as: B. Wang, et al., Indoor positioning via subarea fingerprinting and surface fitting with received signal strength, Pervasive and Mobile Computing (2015), http://dx.doi.org/10.1016/j.pmcj.2015.06.011

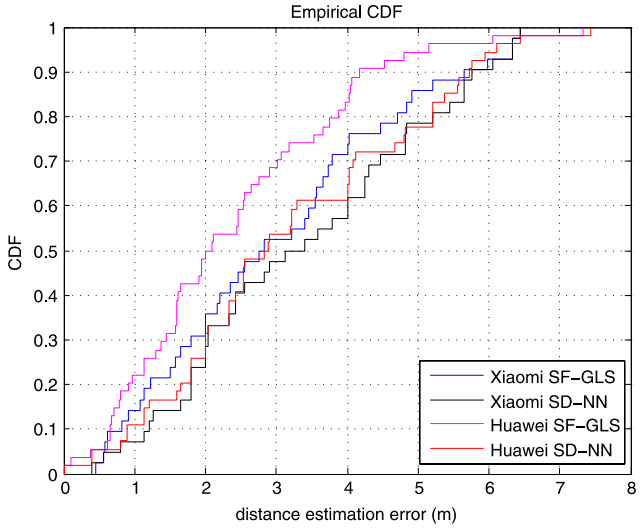

Fig. 14. Experiment results: The CDF of localization error under different device types when using 6 RPs per room.

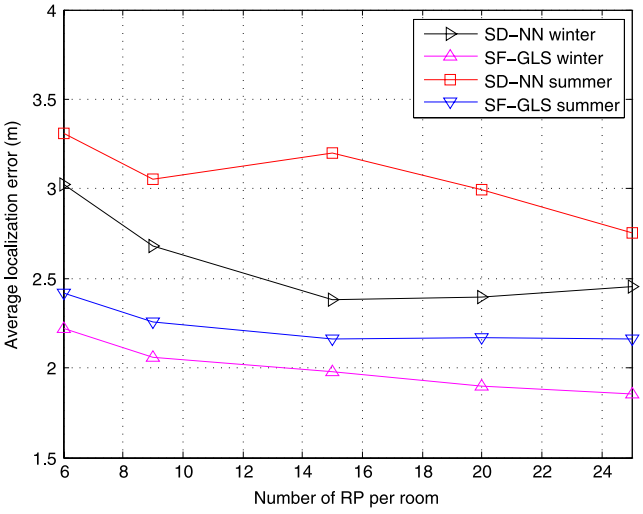

Fig. 15. Experiment results: the RPs' RSS samples in the first batch (winter) are used for fingerprinting and surface fitting. The curve legends 'winter' and 'summer' indicate that the test points sampled in winter and summer, respectively, are used for localization.

test points not sampled in the same season, the SF-GLS still performs better than the SD-NN method when the RPs and test points were sampled in the same day. Take using 6 RPs per room for example, the localization error of SD-NN winter is 3.02 m, but the SF-GLS summer is 2.42 m. The performance improvement is about 20%. This can be even better than SD-NN winter when adopt 25 RPs per room. So our proposed method is more environmental change tolerant.

Next, we use different devices to further study the robustness of our method. Test points sampled in summer by Xiaomi 1S and Huawei U8860 are used to conduct localization. From Fig. 16(a), we can find that the SF-GLS method shows a great advantage than the SD-NN method for both two devices considering environmental change. The average localization errors of SF-GLS are mainly between 2.1 and 2.5 m, while those of SD-NN are mainly between 3.0 and 3.3 m for the two devices. Fig. 16(b) gives the CDF of localization error under different device types. It shows that the median error of SF-GLS and SD-NN for Xiaomi 1S is 2.09 and 3.26 m, and for Huawei U8860 is 2.13 and 2.86 m. The improvement of localization accuracy for the two devices is 36% and 26%, respectively. The reason for its robustness to device diversity might be explained as follows. Notice that a fitted surface not only provides the values of the RSS distribution, but also describes the RSS change pattern. It has been reported that there may exist some linear relation between two different devices RSS measurement [29,30]. This indicates that the RSS measured by device type A might be linearly transformed to the RSS measurements by another device type B. So if the fitted surface is made from device type A, it may be linearly transformed to the fitted surface by device type B. The main difference of the two surfaces might be a same offset across all locations. Therefore, when using the NN algorithm, it introduces a same distance offset to all fitted locations, and still the location with the least distance will be selected. In short,

Please cite this article in press as: B. Wang, et al., Indoor positioning via subarea fingerprinting and surface fitting with received signal strength, Pervasive and Mobile Computing (2015), http://dx.doi.org/10.1016/j.pmcj.2015.06.011

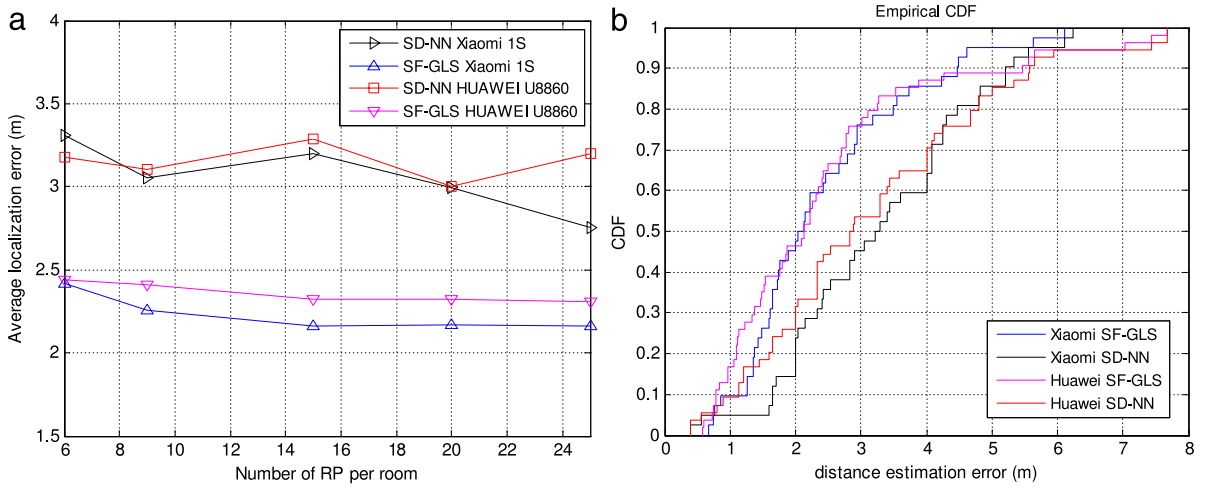

Fig. 16. Experiment results: (a) localization performance comparison when the RPs were sampled in winter by one device, but test points were sampled in summer by two different devices. (b) The CDF of localization error under different device types when using 6 RPs per room.

the experiment results indicate that the SF-GLS method is more robust than the traditional fingerprinting-based method, in terms of graceful performance degradation in different environment conditions and heterogeneous devices types.

5.4. Complexity discussion

Finally, we discuss the online phase complexity of our proposed methods and the traditional fingerprinting method. For the classic NN localization, its complexity is $O(N)$, where N is the total number of fingerprints to be compared in a given indoor environment. After applying the subarea division scheme, the complexity of SD-NN becomes $O(K + N_{subarea})$, where K is the total number of subareas and $N_{subarea}$ is the largest number of RPs in some subarea. In this paper, $N_{subarea}$ is equal to $\frac{N}{K}$. So it can be seen that the subarea division can help to reduce complexity for the traditional NN method. For the ELS method, the complexity is also dependent on the largest number of grid points in some subarea, denoted by $O(K + N_{grid})$. Usually, N_{grid} is much larger than $N_{subarea}$. So the complexity of the ELS is higher than the NN. For the GLS method, we use $O(K + N_{subarea} + t_{max} \times B)$ to denote its complexity, where B represents the complexity of finding the next search point when conducting the iterative search, that is, the computation complexity from line-4 to line-11 in the GLS algorithm description. The complexity of the GLS method is higher than the SD-NN. Given the prominent improvement of GLS localization accuracy over the SD-NN, such moderately increased complexity may be acceptable.

6. Conclusion

In this paper, we have proposed a novel indoor localization scheme based on subarea determination and surface fitting. The whole environment can be divided into some subareas according to the indoor layout. In the offline phase, a fingerprint is first created for each subarea, and several RSS spatial distribution functions are then constructed for each subarea based on surface fitting technique. In the online phase, a target is first determined to which subarea it belongs, and its location is then found by the proposed location search algorithms. Our simulation and experiment results show that for the same RP granularity, the proposed can achieve on average 10% and 22% localization accuracy improvements by using the two proposed localization algorithms respectively, compared with the classical nearest neighbor-based fingerprinting method. In other words, to achieve the same localization performance, our methods can greatly save time and labor for doing field measurements.

We close the paper with some discussions about future work. Recently, some fingerprint crowdsourcing-based localization systems have been proposed [31], where the fingerprints are collected by crowds at unspecified locations. Different from the RP-based fingerprint collection, fingerprint crowdsourcing helps to relieve the burden of site survey. On the other hand, the crowdsourcing approach is not likely to provide the exact location information for a RSS measurement, compared with the RP-based site survey approach. Therefore, it is worth of studying to combine the benefits of both fingerprint crowdsourcing and surface fitting. In our future work, we will study how to build fitted surface from crowdsourced fingerprints.

Acknowledgment

This work is partly supported by the National Natural Science Foundation of China (Grant No. 61371141).

Please cite this article in press as: B. Wang, et al., Indoor positioning via subarea fingerprinting and surface fitting with received signal strength, Pervasive and Mobile Computing (2015), http://dx.doi.org/10.1016/j.pmcj.2015.06.011

References

[1] Y. Kim, H. Shin, Y. Chon, H. Cha, Smartphone-based Wi-Fi tracking system exploiting the RSS peak to overcome the RSS variance problem, Pervasive Mob. Comput. 9 (3) (2013) 406–420.
[2] T. Higuchi, H. Yamaguchi, T. Higashino, Context-supported local crod mapping via collaborative sensing with mobile phones, Elsevier Pervasive Mob. Comput. 13 (2014) 26–51.
[3] P. Bahl, V.N. Padmanabhan, Radar: An in-building RF-based user location and tracking system, in: IEEE INFOCOM, vol. 2, 2000, pp. 775–784.
[4] M. Bshara, U. Orguner, F. Gustafsson, L.V. Biesen, Fingerprinting localization in wimax networks based on received signal strength measurements, IEEE Trans. Veh. Technol. 59 (1) (2010) 283–294.
[5] C.-Y. Shih, L.-H. Chen, G.-H. Chen, E.-K. Wu, M.-H. Jin, Intelligent radio map management for future WLAN indoor location fingerprinting, in: IEEE Wireless Communications and Networking Conference, WCNC, 2012, pp. 2769–2773.
[6] S.-H. Fang, T.-N. Lin, P.-C. Lin, Location fingerprinting in a decorrelated space, IEEE Trans. Knowl. Data Eng. 20 (5) (2008) 685–691.
[7] B. Li, Y. Wang, H. Lee, A. Dempster, C. Rizos, Method for yielding a database of location fingerprints in WLAN, IEE Proc.—Commun. 152 (5) (2005) 580–586.
[8] X. Chai, Q. Yang, Reducing the calibration effort for location estimation using unlabeled samples, in: IEEE International Conference on Pervasive Computing and Communications, PerCom, 2005, pp. 95–104.
[9] R.W. Ouyang, A.K.-S. Wong, C.-T. Lea, M. Chiang, Indoor location estimation with reduced calibration exploiting unlabeled data via hybrid generative/discriminative learning, IEEE Trans. Mob. Comput. 11 (11) (2011) 1613–1626.
[10] J.J. Pan, S.J. Pan, Jie Yin, L.M. Ni, Q. Yang, Tracking mobile users in wireless networks via semi-supervised colocalization, IEEE Trans. Pattern Anal. Mach. Intell. 34 (2012) 587–600.
[11] X. Chai, Q. Yang, Reducing the calibration effort for probabilistic indoor location estimation, IEEE Trans. Mob. Comput. 6 (2007) 649–662.
[12] M. Lee, D. Han, Voronoi tessellation based interpolation method for Wi-Fi radio map construction, IEEE Commun. Lett. 16 (2012) 404–407.
[13] B. Dawes, K.-W. Chin, A comparison of deterministic and probabilistic methods for indoor localization, Elsevier J. Syst. Softw. (2010).
[14] V. Honkavirta, T. Perala, S. Ali-Loytty, R. Piche, A comparative survey of WLAN location fingerprinting methods, in: IEEE Workshop on Positioning, Navigation and Communication, WPNC, 2009, pp. 243–251.
[15] T. Roos, P. Myllymäki, H. Tirri, P. Misikangas, J. Sievänen, A probabilistic approach to WLAN user location estimation, Springer Int. J. Wirel. Inf. Netw. 9 (3) (2002) 155–164.
[16] J.J. Pan, J.T. Kwok, Q. Yang, Y. Chen, Multidimensional vector regression for accurate and low-cost location estimation in pervasive computing, IEEE Trans. Knowl. Data Eng. 18 (2006) 1181–1193.
[17] S.-P. Kuo, Y.-C. Tseng, Discriminant minimization search for large-scale RF-based localization systems, IEEE Trans. Mob. Comput. 10 (2) (2011) 291–304.
[18] Y. Chen, Q. Yang, J. Yin, X. Chai, Power-efficient access-point selection for indoor location estimation, IEEE Trans. Knowl. Data Eng. 18 (7) (2006) 877–888.
[19] S.-P. Kuo, B.-J. Wu, W.-C. Peng, Y.-C. Tseng, Cluster-enhanced techniques for pattern-matching localization systems, in: IEEE Internatonal Conference onMobile Adhoc and Sensor Systems, MASS, 2007, pp. 1–9.
[20] M.A. Youssef, A. Agrawala, A.U. Shankar, Wlan location determination via clustering and probability distributions, in: Proceedings of the First IEEE International Conference on Pervasive Computing and Communications, PerCom, 2003, pp. 143–150.
[21] Y. Mo, Z. Cao, B. Wang, Occurrence-based fingerprint clustering for fast pattern-matching location determination, IEEE Commun. Lett. 16 (12) (2012) 2012–2015.
[22] X.-C. Liu, S. Zhang, Q.-Y. Zhao, X.-K. Lin, A real-time algorithm for fingerprint localization based on clustering and spatial diversity, in: IEEE International Congress on Ultra Modern Telecommunications and Control Systems and Workshops, UMTCSW, 2010, pp. 74–81.
[23] V. Weiss, L. Andorb, G. Rennera, T. Varady, Advanced surface fitting techniques, Elsevier Comput. Adided Goem. Design 19 (1) (2002) 19–42.
[24] R.J. Renka, Multivariate interpolation of large sets of scattered data, ACM Trans. Math. Softw. 14 (2) (1988) 139–148.
[25] M. Gasca, T. Sauer, Polynomial interpolation in several variables, Adv. Comput. Math. 12 (4) (2000) 377–410.
[26] Y.-C. Chang, N-dimension golden section search: Its variants and limitations, in: IEEE 2nd International Conference on Biomedical Engineering and Informatics, 2009, pp. 1–6.
[27] R. de Francisco, Indoor channel measurements and models at 2.4 ghz in a hospital, in: IEEE Global Telecommunications Conference, GLOBECOM, 2010, pp. 1–6.
[28] B. Joshua, The truth about 802.11 signal and noise metrics, 2004.
[29] J. geun Park, D. Curtis, S. Teller, J. Ledlie, Implications of device diversity for organic localization, in: IEEE Infocom, 2011, pp. 3182–3190.
[30] M. Lee, S.H. Jung, S. Lee, D. Han, Elekspot: A platform for urban place recognition via crowdsourcing, in: IEEE/IPSJ 12th International Symposium on Applications and the Internet, SAINT, 2012, pp. 190–195.
[31] A.M. Hossain, W.-S. Soh, A survey of calibration-free indoor positioning systems, Comput. Commun. (2015) 1–13 http://dx.doi.org/10.1016/j.comcom.2015.03.001.

Please cite this article in press as: B. Wang, et al., Indoor positioning via subarea fingerprinting and surface fitting with received signal strength, Pervasive and Mobile Computing (2015), http://dx.doi.org/10.1016/j.pmcj.2015.06.011